02-16-03

On the 53 MHz Tevatron cavity properties.

Cristian Boffo, Ivan Gonin, Timergali Khabiboulline, Gennady Romanov

A series of RF and acoustic measurements and numerical simulations on the 53 MHz Tevatron accelerating cavity RF properties has been done in the course of a particle losses study at Tevatron. The work has been emphasized on RF and acoustic noise study. This report is a summary of the results and includes some general considerations as well.

The Modes

To have a better understanding of Tevatron cavity RF properties it was decided to supplement existing experimental data (D.Sun, C.-Y.Tan) with comprehensive simulation of the cavity-3/4λ transmission line system. A solid model of the system has been built with minor simplifications of the cavity geometry. Only one simplification is important in some way: an absence of absorbing material in the model makes a quality factor value of the appointed modes uncertain. The solid model of the system is shown in Fig.1.

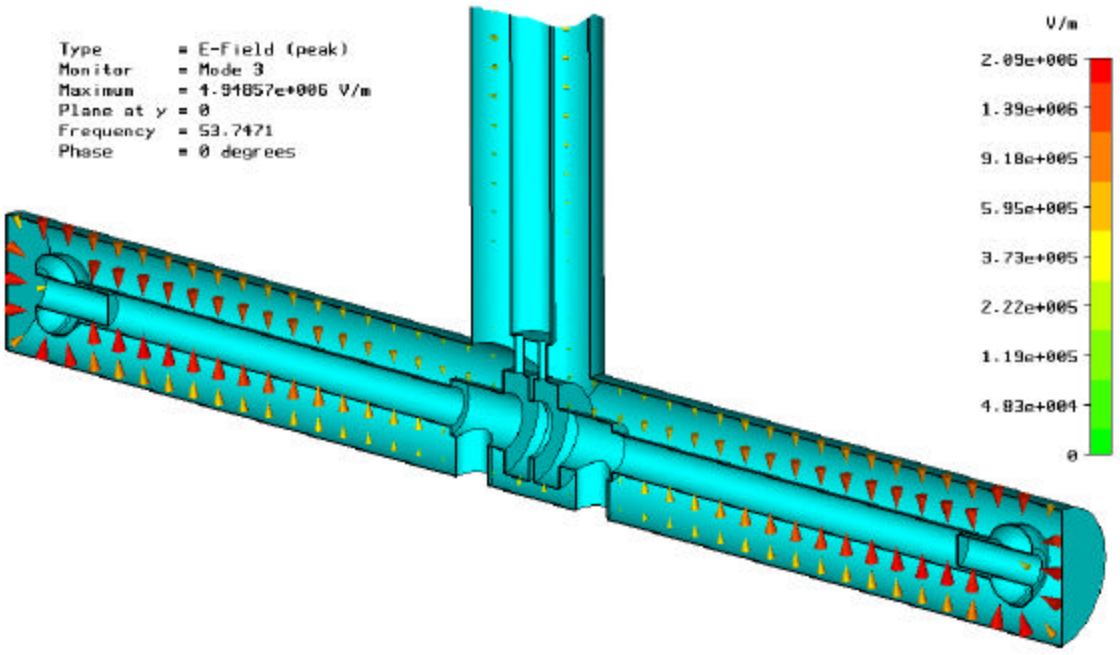

Fig.1 Solid model of Tevatron cavity with transmission line.

The simulations have been made with Omega3P and crosschecked with HFSS and Microwave Studio calculations. The frequencies of the modes are shown in Fig.2 and accompanied with experimental data obtained by D.Sun, C.-Y.Tan, and G.Romanov as far as it was possible to identify the experimental modes.

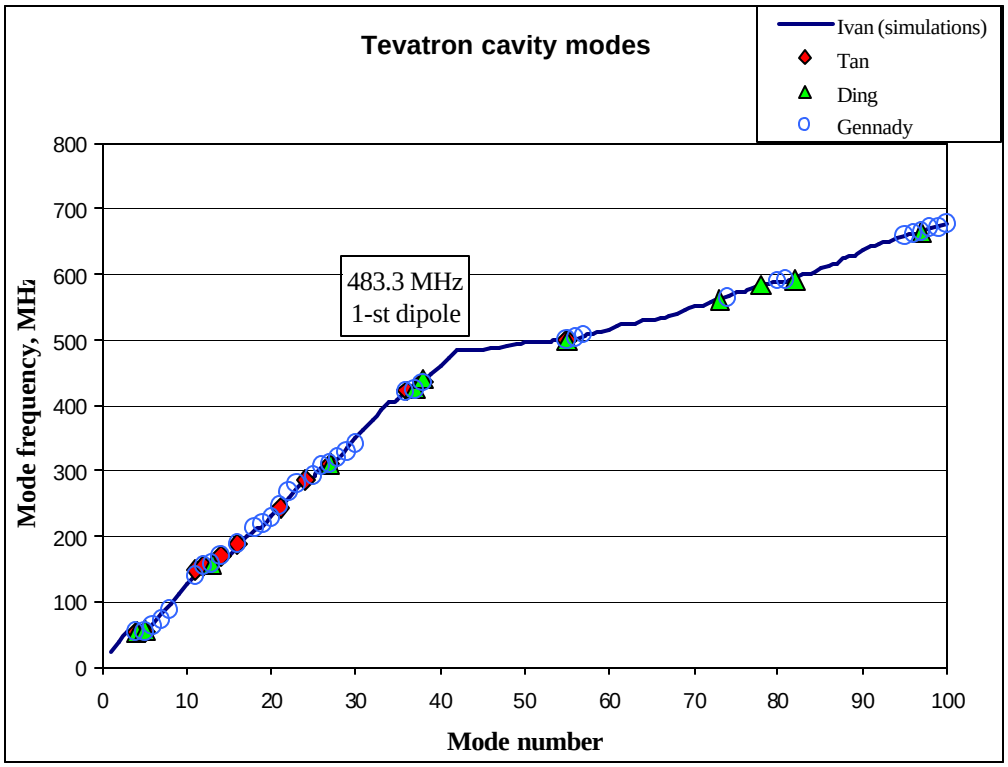

Fig.2. Mode frequencies.

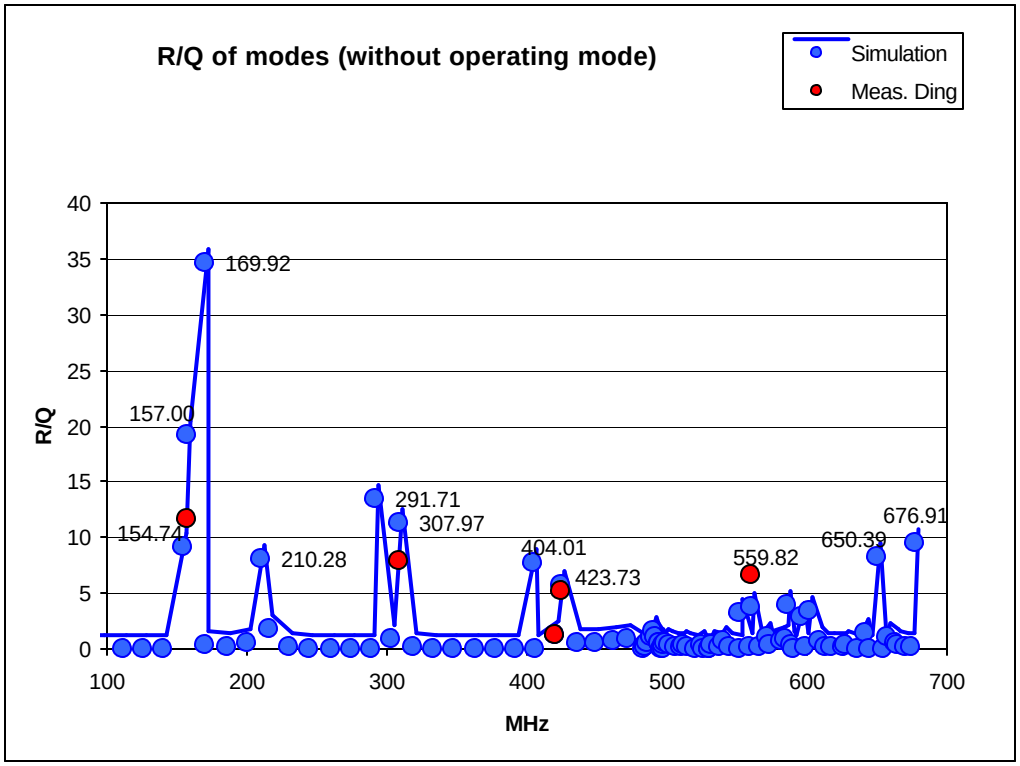

Fig.3. Calculated R_s/Q ratio.

Important parameter R_s/Q has been calculated for all modes. For operating 53 MHz mode calculated R_s/Q = 170 Ω while the design value is 150 Ω and the prototype cavity value is 170 Ω [3]. D.Sun's measurements of the test cavity show R_s/Q = 110 Ω. The result for the rest of modes is given in Fig.3.

It should be mentioned that the modes in which $H_\varphi(z)$ distribution is even function (an example of the distribution is shown in Fig. 4) must be well damped by the absorber in the middle of cavity. So, the high R_s/Q ratio does not mean high shunt impedance value for real cavity. For example, for 170 MHz mode calculated quality factor is Q = 18000, and measured Q value is ≈ 200, so the mode is well damped.

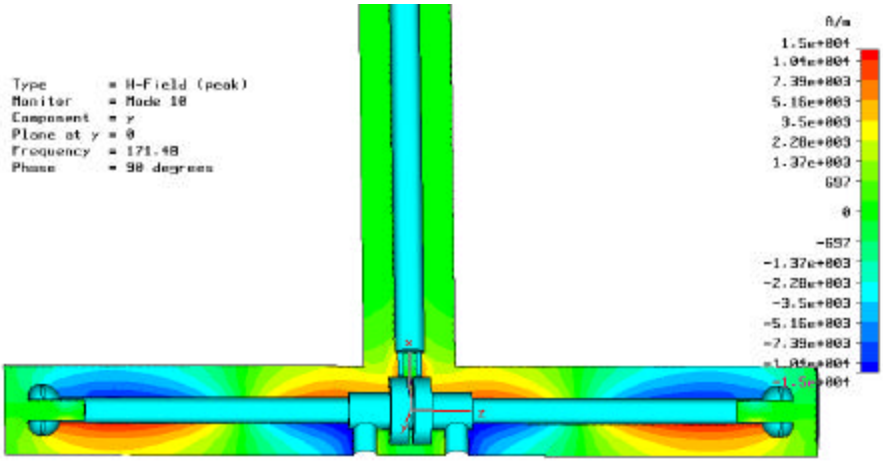

Fig.4. 170 MHz mode, H-field.

Another general remark should be done about dipole and quadrupole modes. The Tevatron cavities have essential azimuth asymmetry mostly due to the central electrode supports. As a result of that some of the multipole modes have strong asymmetry of $E_z(x,y)$ distribution in the accelerating gap (Fig. 5).

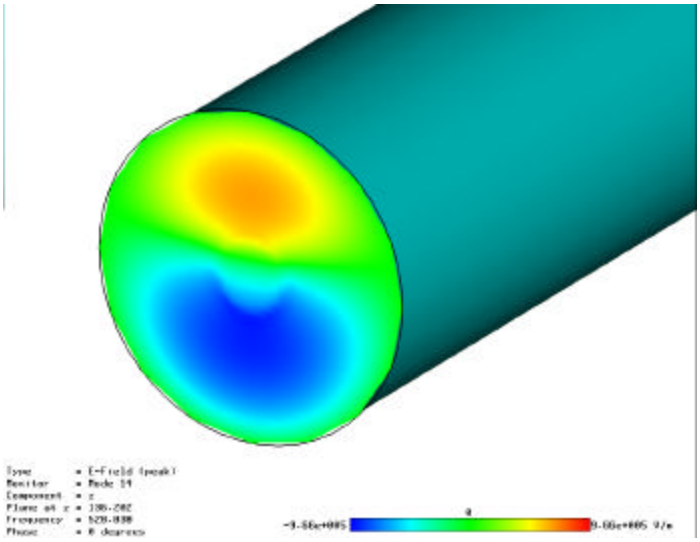

Fig.5. Dipole mode field distribution asymmetry ($E_z(x,y)$ in the accelerating gap).

The complete table of the Tevatron cavity simulation data is given in Appendix A.

The low frequency RF noise.

The low frequency RF noise of 35-37 Hz found in Tevatron RF system has been associated presumably with mechanical vibrations (microphonics) somewhere in or around accelerating cavity assemblies [1,2]. The plots below demonstrate typical measurements made then in a course of low frequency RF noise study.

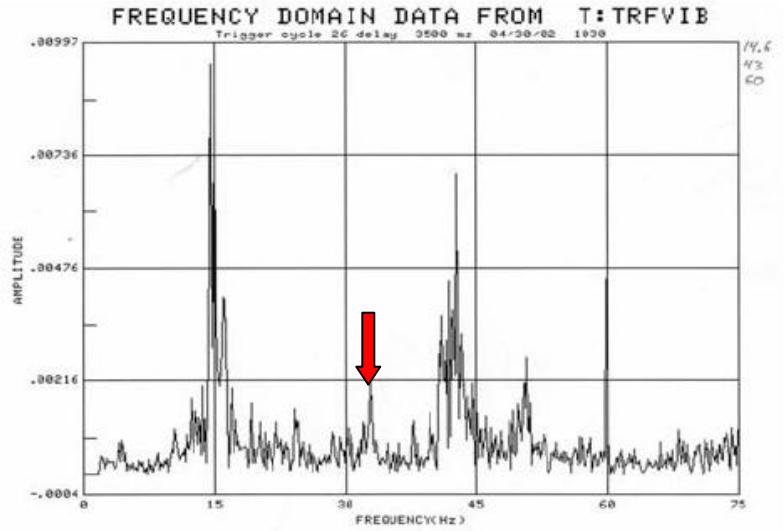

Fig. 6: Spectra of longitudinal mechanical vibrations on one of the RF cavities.

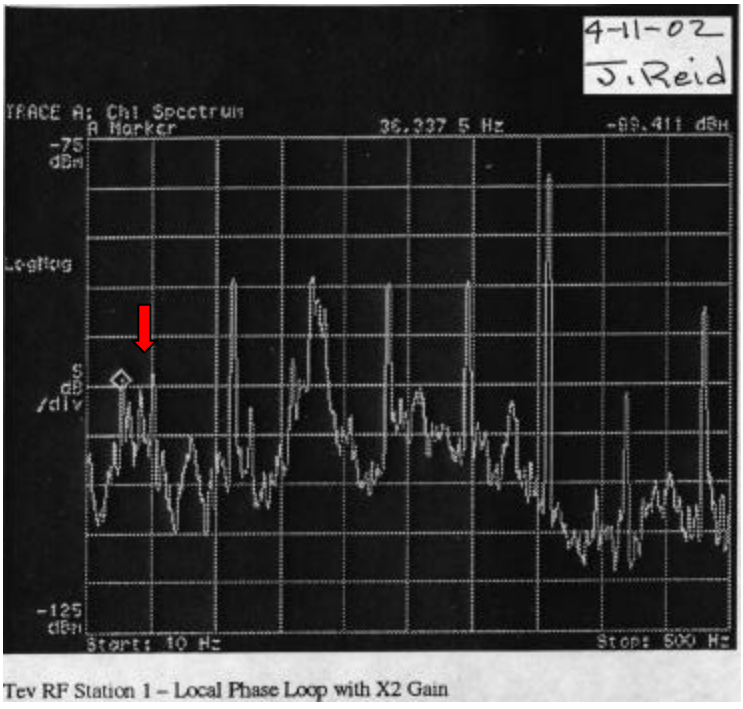

Fig.7. Phase noise in Local Phaselock Loop, Tev RF Station 1.

Our experimental work went on the supposition (G.Romanov) that the source of the 35-37 Hz RF noise is the mechanical vibrations of the central electrodes driven by cooling water. The simulations and subsequent acoustic and RF measurements on the test cavity and the operating ones confirmed this supposition and established the main facts:

1. The mechanical vibrations and RF noise (amplitude and phase) are strongly correlated at frequency under interest.
2. The cooling water flowing inside central electrodes is a main driving force for their mechanical vibrations along with a background noise outside cavities (the heaters first of all).

Complete set of all measurements deserves separate consideration and analysis (prepared and distributed by T.Khabiboulline).

Mechanical vibration simulations

The central electrode in Tevatron accelerating cavity actually is a pretty long tube beam with rigid supports and links in the middle of it. Such a cantilever beam usually can be a good oscillator (like a piece of tuning fork). As mentioned above the central electrode as a mechanical oscillator has got a driving force – cooling water flowing inside it.

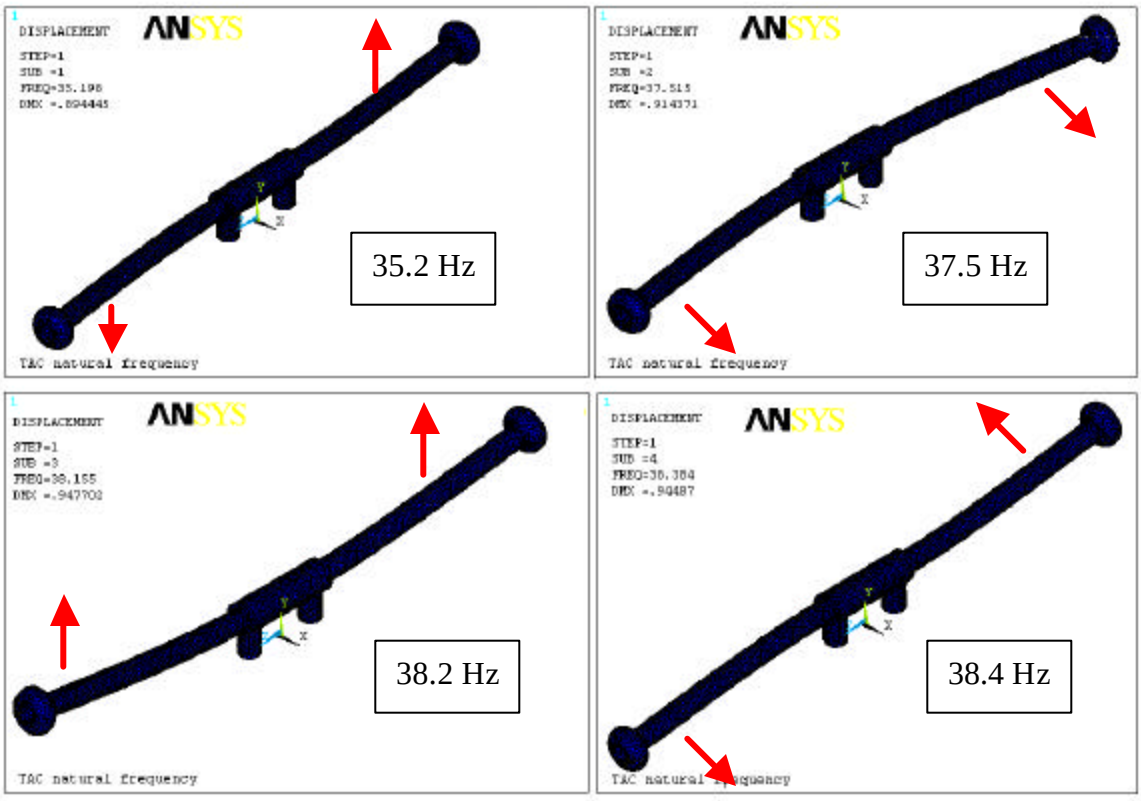

Fig.8. The modes of the central electrode mechanical vibrations (I.Gonin)

A solid model of the central electrode design has been built and a simulation of mechanical vibrations has been performed for two cases. In one case a material of solid

model was copper, and stainless steel in other case. The simulations were done without cooling water inside electrode. The lowest natural frequencies of the central electrode construction are given in a table:

	Mode 1	Mode 2	Mode 3	Mode 4
Copper	35.2 Hz	37.5 Hz	38.2 Hz	38.4
Steel	48.9 Hz	52.1 Hz	53 Hz	53.3 Hz

The modes of mechanical vibrations are shown in Fig.8.

So, the simulated frequencies of mechanical vibrations in a case of copper central electrode are in a close agreement with the measured RF and acoustic noise frequencies. For us it has been a first indication that the central electrode mechanical vibrations may be a cause of RF noise.

Bent central electrode and RF parameters.

A cavity with bent central electrode has been simulated to estimate amplitude of the central electrode vibrations and vibration's influence on RF parameters. Only a half of cavity without transmission line was simulated to increase accuracy of calculations (Fig.9). The curvature of central electrode axis is a regular arc. It seems to be a good enough approximation of small real sinusoidal deformations of electrode during vibrations. Only horizontal deformations have been considered because pick-up electrodes are in horizontal plane and sensitive to these deformations.

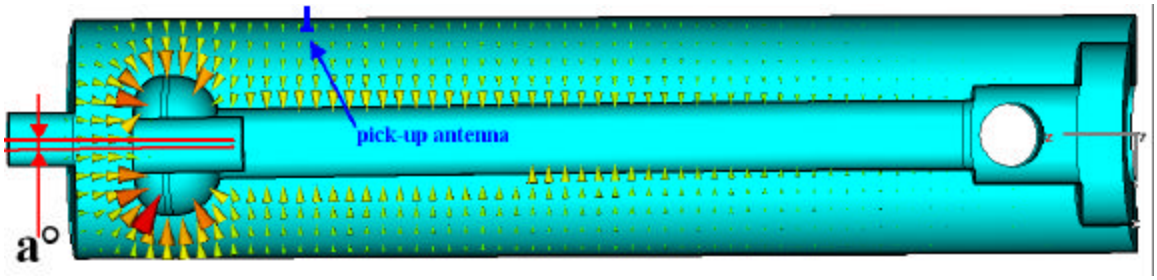

Fig.9. A cavity with bent central electrode.

An angle $a°$ between cavity axis and electrode axis (angle of bend) is a convenient parameter of deformations.

From the RF noise point of view two cavity parameters are important: 1) modulation of resonant frequency of cavity that produces amplitude and phase modulation of accelerating field, and 2) electric field level modulation in pick-up electrode area. The latter has nothing to do directly with particle acceleration, but it is very important as the only signal for the feedback systems. The parameters are considered as a function of bend $a°$. Also a distortion of accelerating field distribution in a gap due to the central electrode bend may be important for acceleration process.

1. A cavity resonance frequency depends strongly on accelerating gap geometry where an electric field has the highest value. Obviously the bent electrodes changes integrated capacitance of the accelerating gaps, so cavity resonant frequency changes too. For small

bend angles the cavity resonance frequency deviation as a function of bend can be described with quite sufficient accuracy by (see also Fig.10)

$$f = a^{2}, \qquad (1)$$

where f is the resonance frequency deviation in kHz, a = 79, - a bend angle in degrees.

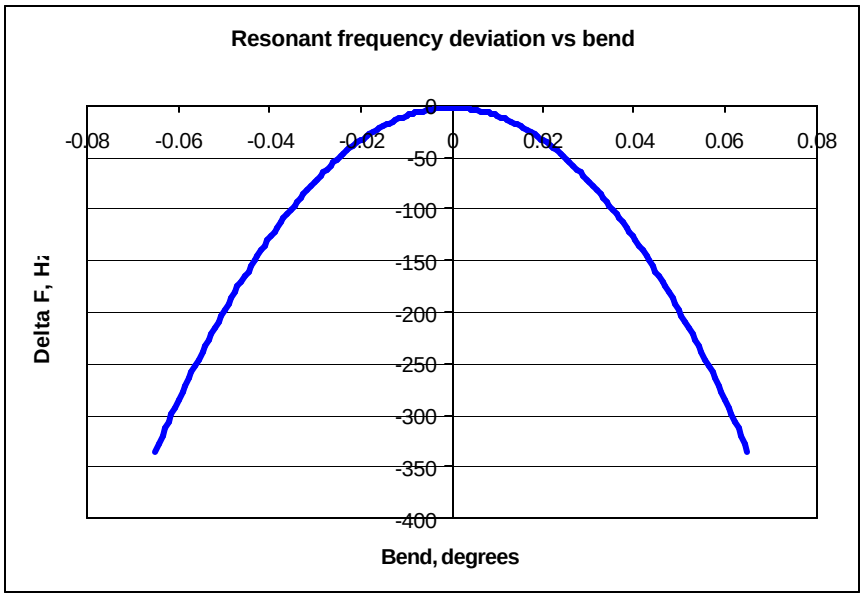

Fig.10. Cavity resonant frequency deviation vs central electrode bend

2. The central electrode bent horizontally creates a field asymmetry in the pick-up electrode plane (Fig. 11):

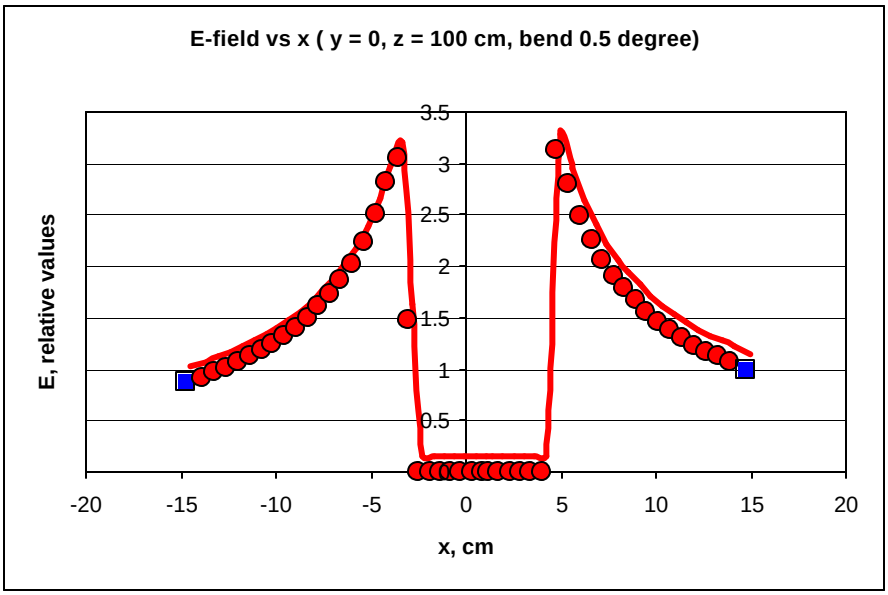

Fig.11. E-field distribution in the pick-up electrode plane with bent central electrode.

This field asymmetry is seen by a pick-up electrode (and feedback system) as a component of amplitude modulation of field. An electric field value deviation in the pick-up electrode area (actually amplitude modulation of the pick-up signal) is a linear function of bend:

$$E/E = b \quad , \qquad (2)$$

where E/E is a relative deviation of field value, coefficient b = 0.154. The function is shown in Fig.12.

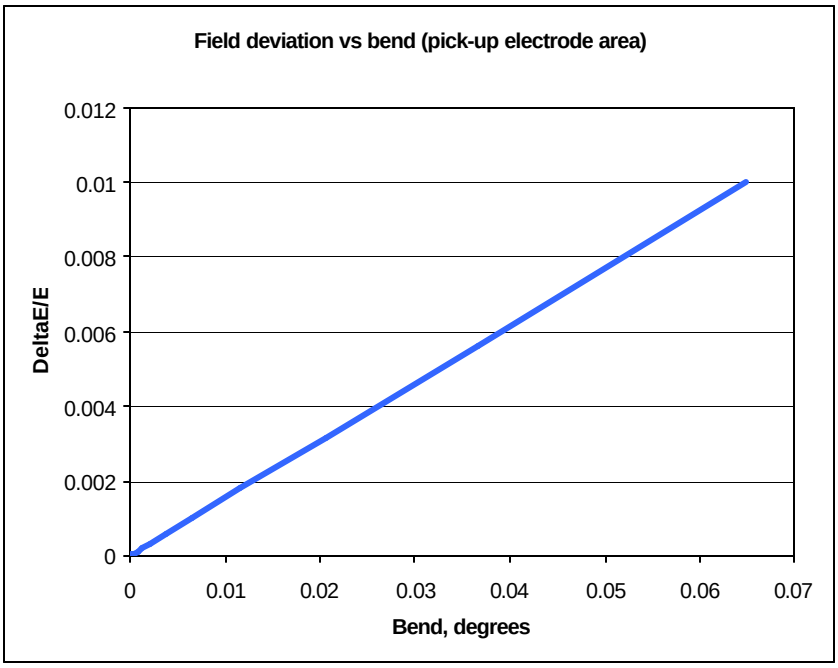

Fig.12. Relative field variation at a pick up electrode vs bend.

These simulations of basic cavity parameters were made with the use of two codes – Microwave Studio and HFSS. In Microwave Studio model the deformed central electrode has a shape of regular arc, while in HFSS model the central electrode is just tilted remaining straight. So, we have to use a displacement of the electrode head as an independent variable instead of "bend angle" and "tilt angle" to compare the results (though the displacement is not an equivalent parameter for both models anyway). Replacing by x in mm in the formulas above, we get the new coefficients we can compare:

	a	b
HFSS	890	0.0117
Microwave Studio	614	0.0136

A remark must be done that the value of coefficient **a** is calculated for both electrodes deformed equally (a symmetry plane has been used for both simulations). If only one electrode is deformed then the coefficient **a** should be multiplied by a factor of 0.7.

3. The central electrode bend creates also accelerating field asymmetry in the gap:

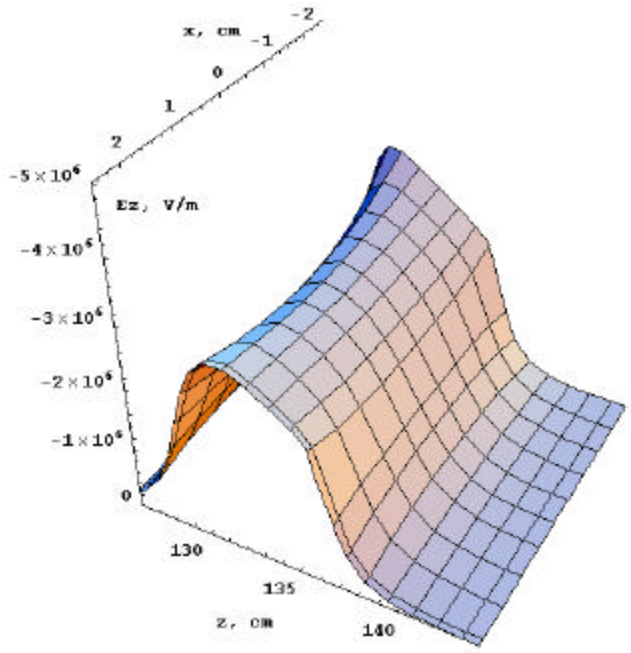

Fig.13. Field distribution in the gap $E_z(x,0,z)$. (Stored energy 1 J, 0.5° bend).

The field distributions on the axis and the boundaries of useful aperture (assumed ± 2 cm) in plane y=0 are given in Fig. 14.

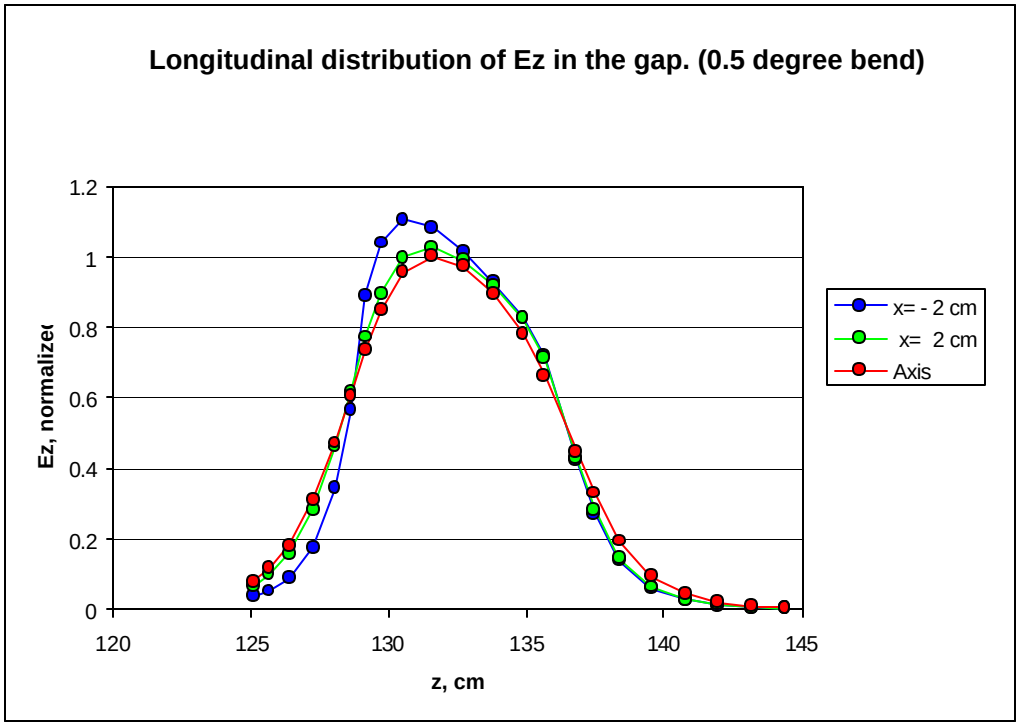

Fig.14.

The difference between peak values is pretty noticeable (≈ 8% for the 0.5° bend), but the maximal difference between integrated voltage gains along specified lines is not so drastic – only 0.5% for the same 0.5° bend. The difference between voltage gains along boundary lines is even less (see Fig.15).

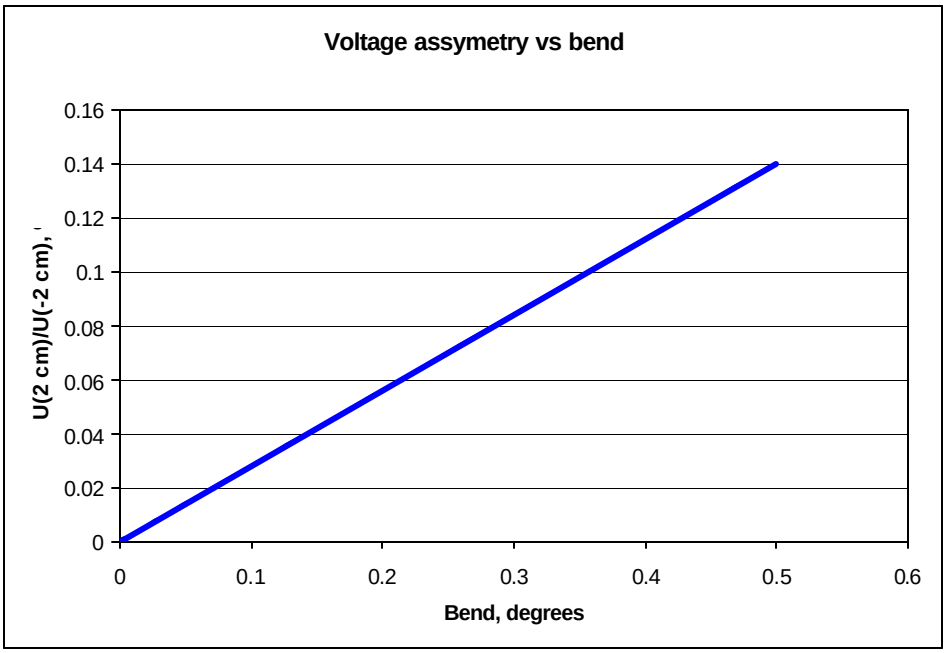

Fig. 15. Voltage asymmetry at the boundaries of useful aperture vs bend.

So, taking into account that the estimated mechanical vibration amplitude is < 0.005 , the field distribution variable asymmetry in the gaps is expected to be quite small < 0.0015%.

Mechanical vibrations to RF noise transformation.

Modulation of cavity resonant frequency produces modulation of phase and amplitude of electromagnetic field oscillations.

1. For small frequency deviations a phase shift can be estimated as

$$\varphi \approx 2\,\Delta f/f\,Q, \qquad (3)$$

where φ is a phase shift, Q is a cavity quality factor, Δf/f –relative resonant frequency deviation .

The sensitivity of resonant frequency to the central electrode bend is low around zero bend point and resonant frequency modulation does not seem to be a problem in a case of perfect axial symmetrical cavity. But the central electrodes can have “natural” bends in any plane that could occur during manufacturing and installation. In this case of “permanent initial bend” a sensitivity of resonant frequency to small bend deviations (vibrations) is higher and estimation is

$$f = (2a \quad + a^{2})f, \qquad (4)$$

where is an initial bend angle, - small bend deviation from initial bend of angle , f

is difference between the resonant frequency at bend angle and the resonant frequency at bend + (see also Fig.16).

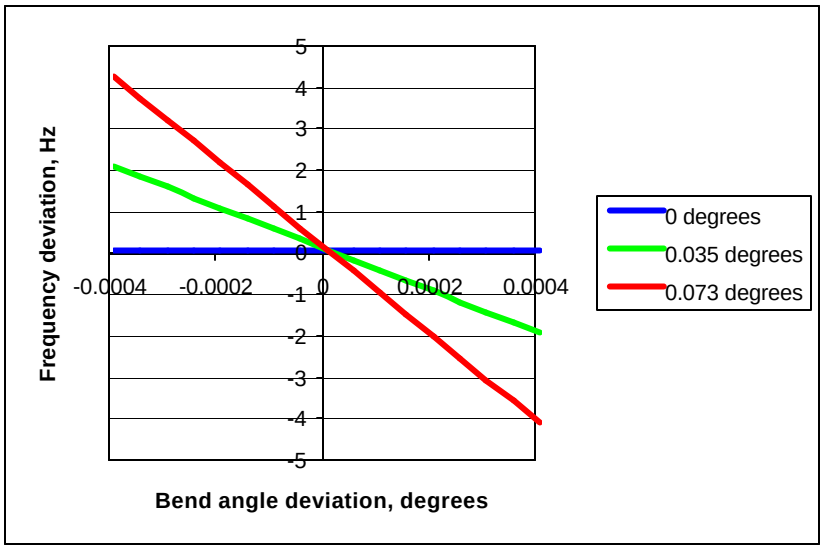

Fig.16. Resonant frequency deviation vs bend deviation at different angles of permanent initial bend (0, 0.035 and 0.073 degrees).

Then estimation for phase shift enhanced by initial permanent central electrode bend is

$$\varphi \approx 2\,Q\,(2a \quad + a^{2})/f, \qquad (4)$$

where Q is cavity quality factor (7 000 assumed).

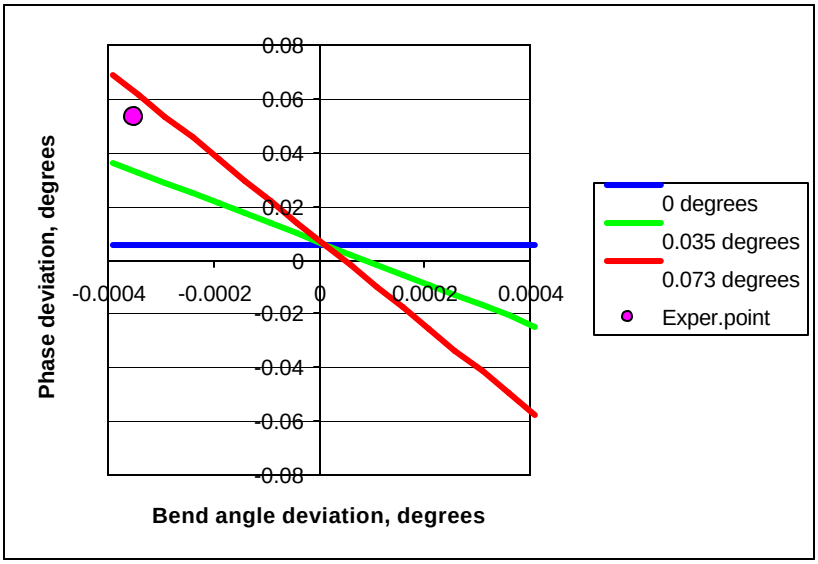

Fig.17. Phase deviations vs bend deviations at different angles of permanent initial bend (0, 0.035 and 0.073 degrees).

2. Amplitude modulation of electromagnetic field produced by resonant frequency modulation is negligible in perfect cavity even if central electrode is bent. In case of small bent angle modulations estimation for amplitude modulations is

$$E/E = - 2 Q^2 (2a \quad + a \quad ^2)^2/f^2 \qquad (5)$$

The result of estimations is given in Fig.18 just for speculative interest.

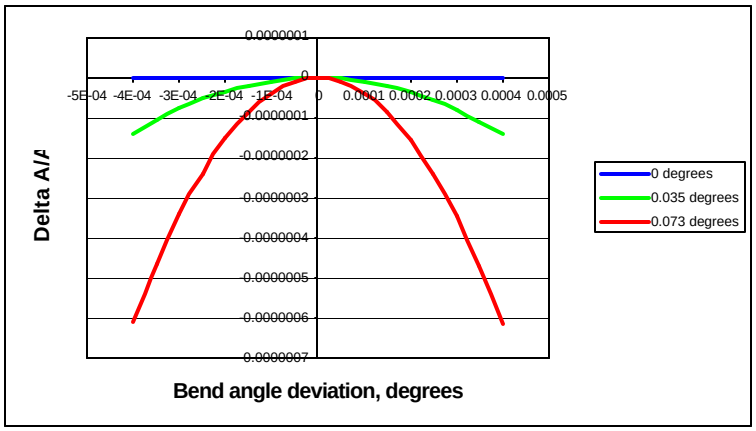

Fig.18. Amplitude deviation vs bend angle deviation at different angles of initial bend.

The amplitude modulation can be enhanced if RF power generator frequency and cavity resonant frequency are not equal. The estimation below shows this enhancement:

$$E/E = - 4 Q^2 (\quad f_{gen}/ f) (\quad f/ f) - 2 Q^2 (\quad f/f)^2, \qquad (6)$$

where f_{gen}/f is a generator frequency offset, (f/f) – cavity resonant frequency modulation due to mechanical vibrations.

This estimation works well for generator frequency offset up to 1 kHz. For larger offsets the results of calculations made with the use of exact formulas are shown in Fig.19.

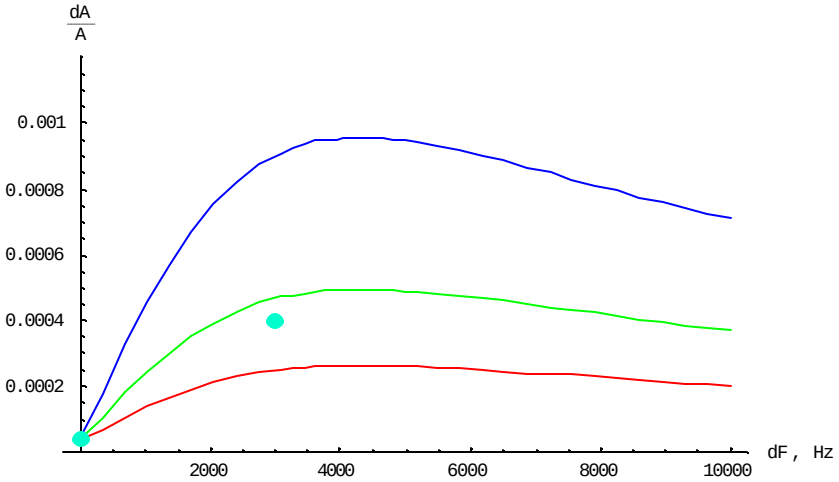

Fig.19. Amplitude modulation vs generator frequency offset at different cavity resonant frequency modulation (red- 2 Hz, green – 4 Hz, blue – 8 Hz, points – measurements).

Below generator frequency offset of 100-150 Hz (the sensible practical values are pretty much below) amplitude modulation of this kind is negligible compare to other source of amplitude modulation.

3. Amplitude modulation due to the field level variation at pick-up electrode area (see expression (2)) seems to be predominant at normal operating conditions. The results presented in Fig.19 include this amplitude modulation component and we may correlate the residual value at dF=0 with this source of modulation. The value of this amplitude modulation depends only on amplitude of mechanical vibrations of one central electrode (see expression (2)). That gives a convenient and reliable way (frequency modulation depends on bends and vibrations of both electrodes, so it is not of unique dependence) to estimate mechanical vibration amplitude. The following table contains some useful conversions made with the simple calculations.

Amplitude noise, dB	, degrees	Displacement, pick-up area, mm	Displacement, Ac. gap area, mm	dE/E pick-up %
-100	6.49E-05	0.000567	0.000737	0.001
-95	0.000115	0.001008	0.00131	0.001778
-90	0.000205	0.001792	0.00233	0.003162
-85	0.000365	0.003187	0.004143	0.005623
-80	0.000649	0.005667	0.007367	0.01
-75	0.001155	0.010077	0.0131	0.017783
-70	0.002053	0.01792	0.023295	0.031623
-65	0.003652	0.031866	0.041426	0.056234
-60	0.006494	0.056666	0.073666	0.1

Amplitude modulation is transformed into phase modulation in phase-lock loop (or feedback loop), because even ideal linear phase-lock loop (PLL) system can generate phase noise responding to amplitude modulation of input signals. It can be shown [4,5] that the rms phase noise in case of perfect phase detector and narrow-band amplitude noise of input signal is given by the simple expression

$$\bar{J}^2 = P_{noise}/2P_{signal}, \text{ (radians}^2\text{)}, \qquad (7)$$

where P_{signal} is the input signal power, and P_{noise} is the total noise power. Taking a reasonable ratio $10\text{Log}(P_{noise}/P_{signal}) = -(70\div90)$ dB one would get an estimation of equivalent input phase variance of 0.013-0.0013°.

Conclusion.

In this study it was found that the primary source of low frequency RF noise in Tevatron accelerating cavities is the mechanical resonant vibrations of the cavity central electrodes driven by cooling water and background acoustic noise. The mechanical vibrations produce cavity resonant frequency modulation and amplitude modulation of pick up electrode signal. Frequency modulation (i.e. phase modulation) is strongly enhanced by axial misalignments of the central electrodes. Amplitude modulation is translated into phase modulation by phase detector.

Basing on the measured amplitude modulation of pick-up signal of –90 dB and phase modulation of –45 dB (low power measurements on station #2) one can get a following table of the estimated parameter deviations assuming symmetrical pattern of vibrations and misalignments for both central electrodes:

Pick-up signal amplitude modulation	$3 \cdot 10^{-3}$ %
Pick-up signal amplitude modulation translated into phase	$1.3 \cdot 10^{-3}$ °
Central electrode bend modulation	$2 \cdot 10^{-3}$ °
Amplitude of mechanical vibrations at pick-up location	1.8 microns
Amplitude of mechanical vibrations at accelerating gap	2.3 microns
Resonant frequency modulation without central electrode bend	$3 \cdot 10^{-3}$ Hz
Phase modulation due resonant frequency modulation without central electrode bend	$\mathbf{4.6 \times 10^{-5}}$ °
Resonant frequency with central electrode bent (real case)	4 Hz
Phase modulation due resonant frequency modulation (real case)	**0.053°**
Central electrodes misalignment	0.073 , 0.83 mm
Resonant frequency shift from optimal value due to central electrodes misalignment	400 Hz

From this table it is seen that the alignment of central electrodes can reduce phase noise significantly. The alignment probably may be done by pushing and pulling the electrodes through the available openings in the cavities using some special tools. A target parameter for the alignment may be maximal resonant frequency of a cavity or minimal RF noise if more sophisticated approach is used.

This study has been done with the great help, support and encouraging from D.Finley, V.Lebedev, J.Reid, V,Shiltsev, J.Steimel, V.Yarba.

References.

1. Tevatron Magnets And Orbit Vibrations V. Shiltsev, T.Johnson, X.L.Zhang, FNAL. Conference?
2. BD. Minutes of March 20,2002 meeting devoted to the study of RF phase and amplitude noise due to microphonics. Present: T. Johnson, V.Lebedev, J. Reid, V. Shiltsev, J. Steimel, C. Tan, D. Wildman.
3. Q.Kerns et all. Energy Saver Prototype Accelerating Resonator. PAC 85, Vancouver, Part I, p. 1852, 1985.
4. Floyd M. Gardner. Phaselock Techniques. John Wiley&Sons, Inc., 1967.
5. Roland E. Best. Phase-Locked Loops. McGraw-Hill, Inc., 1984.

Appendix A

Simulations				Tan		Ding			Test cav. 01.23.03 Gennady	
Mode	Freq. MHz	Q	R/Q Ohm	Freq.	Q	Freq.	Q	R/Q	Freq.	Freq.split.
0	22.228	6565	0.00							
1	37.042	8467	0.00							
2	51.853	10000	0.53							
3	52.871	9282	169.57	53.104	7050	53.114	6523	109.6	53.139	
4	54.319	9940	166.86	54.512	237	56.51	3620	18.81	54.5	
5	66.669	11343	0.01						62.7	
6	81.484	12545	0.00						73.9	84.4
7	96.282	13623	0.00						88	89.3
8	111.080	14653	0.01							
9	125.893	15598	0.02							
10	140.643	16457	0.08	148.77	1391				139	149
11	154.741	15423	9.08	155	780				154	
12	157.000	14422	19.20			158.23	6060	11.68	158	
13	169.920	16977	34.57	170.18	196				170	
14	170.334	18139	0.35							
15	185.058	18901	0.21	186.78	445				188	
16	199.558	19372	0.57							
17	210.276	15274	8.04						211.8	
18	215.946	18688	1.88						219.7	
19	229.944	20873	0.15						229.3	238
20	244.552	21662	0.05	242.33	207				245.1	
21	259.289	22291	0.04						268.1	
22	274.015	22969	0.04						280	
23	288.708	23563	0.07	285.8	75					
24	291.713	21199	13.51						293	
25	303.212	24127	0.89						306	
26	307.968	22217	11.22	311.2	1037	310.7	15923	7.97	310.9	
27	318.433	24652	0.13						318.75	
28	333.026	25303	0.02						329.5	330
29	347.683	25856	0.01						341.2	
30	362.397	26373	0.00							
31	377.027	26857	0.00							
32	391.591	27244	0.00							
33	404.010	22402	7.75							
34	406.041	27529	0.01							
35	419.654	25781	1.26	421	1118				419.74	
36	423.729	25030	5.78			424.25	6394	1.28	423.1	425.2
37	435.088	28630	0.50	437	1571	439.77	13728	5.23	434.26	439.8
38	448.625	28067	0.46							
39	460.937	26667	0.76							
40	471.935	26336	0.84							
41	483.186	32515	0.02							
42	483.825	31936	0.22							

43	483.881	28839	0.35							
44	484.872	32376	0.13							
45	486.312	31811	0.47							
46	487.919	30712	1.11							
47	489.720	29687	1.69							
48	491.845	30629	1.12							
49	494.363	31710	0.51							
50	494.363	31710	0.51							
51	496.187	29838	0.06							
52	496.637	30209	0.08							
53	497.515	29659	0.28							
54	497.868	31014	0.60	499	4158	498.5	8326	0	499.1	
55	501.286	32407	0.31						502.8	
56	505.311	32818	0.21						507.3	
57	509.669	33160	0.16							
58	511.019	30862	0.27							
59	514.566	33384	0.12							
60	519.672	33691	0.08							
61	524.548	31869	0.37							
62	525.207	33954	0.07							
63	529.816	32469	0.00							
64	530.443	33431	0.07							
65	531.683	32841	0.37							
66	537.380	34291	0.10							
67	539.384	32062	0.78							
68	543.992	34618	0.10							
69	550.860	34846	0.07							
70	551.270	31793	3.30							
71	557.971	35151	0.15							
72	559.824	30933	3.86			559.48	13928	6.73		
73	565.404	35419	0.16						564.4	
74	571.237	32054	1.16							
75	573.136	35631	0.31							
76	580.913	35587	0.71							
77	584.797	33082	0.83			583.39	8986	0.11		
78	586.377	33565	3.92							
79	588.646	34745	0.44						588.99	
80	589.561	35869	0.01						590	
81	596.132	29316	2.81			592.39	10402	0.21		
82	599.143	33394	0.23							
83	600.718	27009	3.38							
84	607.959	33406	0.71							
85	613.309	33822	0.24							
86	616.584	35414	0.26							
87	625.692	36209	0.12							
88	627.442	34346	0.43							
89	635.041	36655	0.08							
90	641.111	34847	1.41							

91	644.625	36991	0.06							
92	650.393	33337	8.25							
93	654.376	36927	0.07							
94	657.367	33514	1.05						657.7	
95	662.775	16943	0.61						661.3	663.2
96	664.581	37180	0.28			664.7	13763	0.35	664.79	
97	670.172	34602	0.26						670.13	
98	674.549	38638	0.11						672	
99	676.913	35323	9.56						677.5	